

Retrieval Of Air Quality Using A Newly Simulated Algorithm From Aerosol Optical Depth

H. S. Lim, M. Z. MatJafri and K. Abdullah

*School of Physics,
University of Science Malaysia,
11800 Penang, Malaysia*

*E-mail: mjafri@usm.my, khirudd@usm.my
Tel: +604-6533888, Fax: +604-6579150*

Abstract

A new aerosol retrieval algorithm is presented which computes the air quality at University Sains Malaysia (USM). The algorithm used in this study was derived from the characteristic of the atmospheric effect on remote sensing and applied to the digital camera data. The air quality tested in this study was PM10. The digital images were captured using a normal digital camera, Kodak DC 290 with three visible bands. The digital images were separated into three bands namely red, green and blue bands for multispectral algorithm calibration. Algorithm calibration was performed by using the data provided by Alam Sekitar Sdn. Bhd. (ASMA) acquired simultaneously with digital images. A normalization technique was carried out in this study to ensure the combination of multitemporal data. The acquired PM10 data set was separated randomly into two groups, one was used for algorithm calibration and another one was used for algorithm verification analysis. A high value of correlation was obtained between the retrieved reflectance values and PM10 measurements. This suggests that the application of the generated algorithm on digital camera imagery data is feasible.

Introduction

Aerosols are tiny particles suspended in the air (mostly in the troposphere). Some come from natural sources, such as volcanic eruptions, dust storms, forest and grassland fires, living vegetation and sea spray. About 11 % of the total emitted aerosols in our atmosphere come from human activities, such as the burning of vegetation and fossil fuels and changing the natural land surface cover, which again leads to windblown dust. Yet the human-produced aerosols account for about half of the total effect of all aerosols on incoming sunlight. From a satellite's perspective, aerosols raise the Earth's albedo, or make it appear brighter, by scattering and reflecting sunlight back to a space. The overall effect of these tiny particles is to cool the surface by absorbing and reflecting incoming solar radiation. Aerosol optical thickness is a measure of how much sunlight airborne particles prevent from traveling through a column of atmosphere (King and Herring, 2003). Airborne particulate matter or aerosols, whether anthropogenic or have natural origin constitutes a major environmental issue: At regional level, aerosols are

contributors to visibility degradation (haze) and to acid deposition; at global level that they play a role in climate change (Sifakis and Soulakellis). The direct effect of aerosols is that aerosols directly scatter and absorb the radiation, while the indirect effect is caused by aerosols acting as cloud condensation nuclei (CCN) to change the cloud lifetime (Nakajima, et al., 2001). Air pollution in Asian cities has grown with the progressing industrialization and urbanization. This recent experience in Asia is predated by similar problems in the western countries at early stages of their economic development (*UNEP Assessment Report*).

The objective of this study is to estimate the concentrations of the air pollutant in time and space. We use a normal digital camera, Kodak DC290 to capture digital images of a selected target. This study gives an economical way for estimation air quality at University Sains Malaysia campus, Penang, in local scale. An algorithm was generated based on the aerosol optical depth theory. The algorithm was use to estimate the PM10 measurements. A normalization technique was used in this study for correction of multitemporal data for algorithm calibration.

Remote sensing technique has been widely used for environment pollutant application such as water quality [Dekker, et al., (2002), Tassan, (1993) and Doxaran, et al., (2002)] and air pollutant (Ung, et al., 2001b). Several studies have shown possible relationships between satellite data and air pollution [Weber, et al., (2001) and Ung, et al, (2001a)]. Other researchers used satellite data in such environment atmospheric studies such as NOAA-14 AVHRR (Ahmad and Hashim, 1997) and TM Landsat (Ung, et al., 2001b).

Study Area

The selected air quality station is located in USM campus at longitude of $100^{\circ} 17.864'$ and latitude of $5^{\circ} 21.528'$ (Figure 1). The site consists mainly of undulating land and has many assets that make it an ideal University campus. University Sains Malaysia is situated in the northeast district of Penang island (Figure 1).



Figure 1. Study area and Air Quality Station

Algorithm Model

The atmospheric reflectance due to molecule, R_r , is given by (Liu, et al., 1996) as

$$R_r = \frac{\tau_r P_r(\theta)}{4\mu_s \mu_v} \quad (1)$$

where

τ_r = aerosol optical thickness (Molecule)
 $P_r(\theta)$ = Rayleigh scattering phase function
 μ_v = cosine of viewing angle
 μ_s = cosine of solar zenith angle

We assume that the atmospheric reflectance due to particle, R_a , was also linear with the τ_a of a factor, K_0 . This assumption was reasonable because Liu, et al., (1996) also found the linear relationship between both aerosol and molecule scattering.

$$R_a = K_0 \tau_p + K_1 \quad (2)$$

Atmospheric reflectance was the sum of particle reflectance and molecule reflectance, R_{atm} , (Vermote, et al., 1997).

$$R_{atm} = R_a + R_r \quad (3)$$

where

R_{atm} = atmospheric reflectance
 R_p = particle reflectance
 R_r = molecule reflectance

$$R_{atm} = \left[K_0 \tau_p + K_1 + \frac{\tau_r P_r(\theta)}{4\mu_s \mu_v} \right] \quad (4)$$

The optical depth was given by Camagni and Sandroni, (1983), as equation (5). From the equation, we rewrite the optical depth for particle and molecule as equation (6)

$$\tau = \sigma \rho s \quad (5)$$

where
 τ = optical depth
 σ = absorption
 s = finite path

$$\tau_r = \sigma_r \rho_r s \quad (6a)$$

$$\tau_p = \sigma_p \rho_p s \quad (6b)$$

Equations (6) are substituted into equation (4). The result was extended to a three-band algorithm as equation (7)

Form the equation; we found that PM10 was linearly related to the reflectance for band 1 and band 2. This algorithm was generated based on the linear relationship between τ and reflectance. Retalis et al. also found that the PM10 was linearly related to the τ and the correlation coefficient for linear was better than exponential in their study (overall). This means that reflectance was linear with the PM10.

$$R_{am1} = \left[K_0 \tau_p + K_1 + \frac{\tau_r P_r(\theta)}{4\mu_s \mu_v} \right]$$

$$R_{am} = \left[\sigma_p \rho_p s P_p(\theta) K_0 + 4\mu_s \mu_v K_1 + \frac{\sigma_r \rho_r s P_r(\theta)}{4\mu_s \mu_v} \right]$$

$$R_{am} = \left[\sigma_p A s P_p(\theta) K_0 + 4\mu_s \mu_v K_1 + \frac{\sigma_r G P_r(\theta)}{4\mu_s \mu_v} \right]$$

$$R_{am1} = \left[\sigma_{p1} A s P_{p1}(\theta) K_2 + 4\mu_s \mu_v K_3 + \frac{\sigma_{r1} G P_{r1}(\theta)}{4\mu_s \mu_v} \right]$$

$$R_{am2} = \left[\sigma_{p2} A s P_{p2}(\theta) K_4 + 4\mu_s \mu_v K_5 + \frac{\sigma_{r2} G P_{r2}(\theta)}{4\mu_s \mu_v} \right]$$

$$G = \frac{4\mu_s \mu_v}{\sigma_{r1} P_{r1}(\theta)} \left[R_{am1} - \sigma_{p1} A s P_{p1}(\theta) K_0 - 4\mu_s \mu_v K_1 \right]$$

$$R_{am2} = \sigma_{p2} A s P_{p2}(\theta) K_4 + 4\mu_s \mu_v K_5 + \frac{\sigma_{r2} P_{r2}(\theta)}{4\mu_s \mu_v} \left[\frac{4\mu_s \mu_v}{\sigma_{r1} P_{r1}(\theta)} \left[R_{am1} - \sigma_{p1} A s P_{p1}(\theta) K_0 - 4\mu_s \mu_v K_1 \right] \right]$$

$$R_{am2} = \sigma_{p2} A s P_{p2}(\theta) + 4\mu_s \mu_v K_5 + \frac{\sigma_{r2} P_{r2}(\theta) R_{am1}}{\sigma_{r1} P_{r1}(\theta)} - \frac{\sigma_{r2} P_{r2}(\theta) \sigma_{p1} A s P_{p1}(\theta)}{\sigma_{r1} P_{r1}(\theta)} - \frac{4\mu_s \mu_v K_1 \sigma_{r2} P_{r2}(\theta)}{\sigma_{r1} P_{r1}(\theta)}$$

$$R_{am2} = \frac{(\sigma_{p2} A s P_{p2}(\theta)) (\sigma_{r1} P_{r1}(\theta))}{\sigma_{r1} P_{r1}(\theta)} + \frac{(4\mu_s \mu_v K_5) (\sigma_{r1} P_{r1}(\theta))}{\sigma_{r1} P_{r1}(\theta)} + \frac{\sigma_{r2} P_{r2}(\theta) R_{am1}}{\sigma_{r1} P_{r1}(\theta)} - \frac{\sigma_{r2} P_{r2}(\theta) \sigma_{p1} A s P_{p1}(\theta)}{\sigma_{r1} P_{r1}(\theta)} - \frac{4\mu_s \mu_v K_1 \sigma_{r2} P_{r2}(\theta)}{\sigma_{r1} P_{r1}(\theta)}$$

$$R_{am2} = t_0 A + t_1 R_{am1} + t_3 A + t_4 - t_5$$

$$R_{am2} = (t_0 - t_3) A + t_1 R_{am1} + t_4 - t_5$$

$$(t_0 - t_3) A = R_{am2} - t_1 R_{am1} - t_4 + t_5$$

$$A = e_0 R_{atm1} + e_1 R_{atm2} + e_2$$

$$A = e_0 + e_1 R_{atm1} + e_2 R_{atm2} + e_3 R_{atm3} \quad (7)$$

Where

A = particle concentration (PM10)

G = molecule concentration

R_{atmi} = atmospheric reflectance, $i = 1, 2$ and 3 are the number of the band

e_j = algorithm coefficient, $j = 0, 1, 2$ and 3 are then empirically determined.

Data Analysis and Results

All the image-processing tasks were carried out using PCI EASI/PACE version 6.2 digital image processing software at the School Of Physics, University of Science Malaysia (USM). The digital images were separated into three bands (red, green and blue) for multispectral algorithm analysis. The average DN for each digital image captured at near and far distance from the reference targets were extracted. Digital images captured near to the reference target were corrected using normalization technique. Presumption made in this study was that the digital imagery captured from near to the reference target was not affected by atmosphere scattering.

A red colour paper was stick on the wall of a building as a reference target. The digital image capture near to the reference target at 9.00 a.m on 5 December 2003 was used as reference image. The difference from the DN value was used to correct for each image captured from near to the target. All the DN values of the digital imageries captured from far to the reference were adjusted according to their corresponding difference in the DN values based on the digital images captured from near to the reference target. This normalization technique forced the digital images to have the same illumination condition and the effect due to different solar angle was removed.

All the DN values were then converted into irradiance (equation 1, 2 and 3) using the digital camera coefficients calibrated previously for each bands (Lim, 2003). The irradiances were then converted to reflectance using equation 11 for each band. The solar angles and Earth-Sun distance were calculated corresponding to the acquisition times of the digital images. The mean solar exoatmospheric irradiance values used in this study were $1555 \text{ W/m}^2/\mu\text{m}$, $1843 \text{ W/m}^2/\mu\text{m}$ and $1970 \text{ W/m}^2/\mu\text{m}$ for the red, green and blue bands respectively.

The calibrated digital camera coefficients are

$$y_1 = 0.0005x_1 + 0.0738 \quad (8)$$

$$y_2 = 0.0007x_2 + 0.0517 \quad (9)$$

$$y_3 = 0.0006x_3 + 0.0497 \quad (10)$$

where

- y_1 = irradiance for red band ($\text{Wm}^{-2} \text{nm}^{-1}$)
- y_2 = irradiance for green band ($\text{Wm}^{-2} \text{nm}^{-1}$)
- y_3 = irradiance for blue band ($\text{Wm}^{-2} \text{nm}^{-1}$)
- x_1 = digital number for red band
- x_2 = digital number for green band
- x_3 = digital number for blue band

$$R = \frac{\pi L(\lambda) d^2}{E(\lambda) \cos \theta} \quad (11)$$

where

- $L(\lambda)$ = radiance ($\text{Wm}^{-2} \text{sr}^{-1} \mu\text{m}^{-1}$)
- d = Earth-Sun distance in astronomical units
= $\{1.0 - 0.016729 \cos[0.9856(D-4)]\}$ where (D = day of the year)
- $E(\lambda)$ = mean solar exoatmospheric irradiance ($\text{Wm}^{-2} \mu\text{m}^{-1}$)
- θ = solar Zenith angle (degrees)

Finally, the data were separated into two group, one consisted of 17 data points for algorithm calibration and the other one consisted of 16 data point for verification analysis. Table 1 shows the algorithm calibration coefficient obtained using the generated algorithm. Figure 2 shown the correlation coefficient and RMS error of the measured and estimated PM10 values for calibration analysis. Figure 3 shows the correlation coefficient and RMS error of the measured and estimated PM10 values for verification analysis.

Table 1: The coefficients for the calibrated algorithm

Algorithm Coefficients	Values
e_0	-27.1313
e_1	-8.9957
e_2	-140.4144
e_3	873.4354

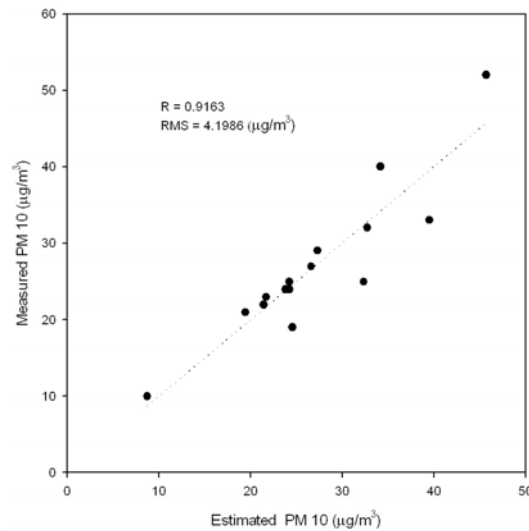


Figure 2: Correlation coefficient and RMS error of the measured and estimated PM10 values for calibration analysis

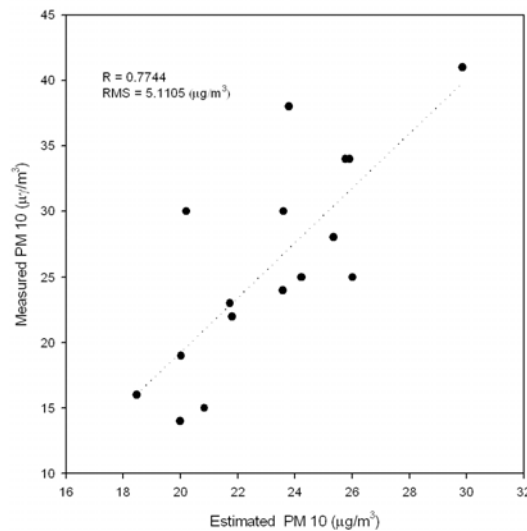


Figure 3: Correlation coefficient and RMS error of the measured and estimated PM10 values for verification analysis

Conclusion

We are quite confident with the result produced by this algorithm after verification analysis. This first application of the generated algorithm illustrates the potential use of digital camera imagery for the PM0 estimation. The high correlation was found between the retrieval reflectance and PM10 values gave an indication of the reliability of the generated algorithm. This study gives an economical way for air quality detection.

Further work will be carried out to improve the normalization technique and more data are required for verification analysis of the generated algorithm.

Reference

Asmala Ahmad, Mazlan Hashim, (2002). Determination of haze using NOAA-14 AVHRR satellite data, [Online] available: <http://www.gisdevelopment.net/aars/acrs/2002/czm/050.pdf>

Camagni, P. and Sandroni, S. (1983) Optical Remote sensing of air pollution, Joint Research Centre, Ispra, Italy, Elsevier Science Publishing Company Inc.

Dekker, A. G., Vos, R. J. and Peters, S. W. M. (2002). *Analytical algorithms for lakes water TSM estimation for retrospective analyses of TM dan SPOT sensor data*. International Journal of Remote Sensing, 23(1), 15–35.

Doxaran, D., Froidefond, J. M., Lavender, S. and Castaing, P. (2002). *Spectral signature of highly turbid waters application with SPOT data to quantify suspended particulate matter concentrations*. Remote Sensing of Environment, 81, 149–161.

King, M. D. and Herring, D. D. (2003) Research (Atmospheric Science), [Online] available: [http://climate.gsfc.nasa.gov/publications/fulltext/Encyclopedia_\(2002\).pdf](http://climate.gsfc.nasa.gov/publications/fulltext/Encyclopedia_(2002).pdf).

Lim, H. S., (2003). Total Suspended Solids Mapping Using Digital Camera Imagery Taken From Light Aircraft. M. Sc. Theses, Unpublished.

Liu, C. H., Chen, A. J. and Liu, G. R. (1996) An image-based retrieval algorithm of aerosol characteristics and surface reflectance for satellite images, International Journal Of Remote Sensing, 17 (17), 3477-3500.

Nakajima, T., Higurashi, A., Kawamoto, K. and Takemura T. (2001) Effects of made-made air pollution on the climate, Present and Future of Modeling Global Environmental Change: Toward Integrated Modeling, pp. 77–87, [Online] available: <http://www.terrapub.co.jp/e-library/toyota/pdf/077.pdf>

Retalis, A., Sifakis, N., Grosso, N., Paronis, D. and Sarigiannis, D. Aerosol optical thickness retrieval from AVHRR images over the Athens urban area, [Online] available: http://sat2.space.noa.gr/rsensing/documents/IGARSS2003_AVHRR_Retalisetal_web.pdf

Sifikis, N. I. and Soulakellis, N. A., Satellite image processing for haze and aerosol mapping (SIPHA): code description and presentation of results, [Online] available: http://www.space.noa.gr/rsensing/documents/IGARSS_2000_web.pdf

Sifakis , Soulakellis and Paronis, (1998) Quantitative mapping of air pollution density using Earth observations: a new processing method and application to an urban area, *International Journal Remote Sensing*, 19(17), 3289 - 3300

Tassan, S. (1997). A numerical model for the detection of sediment concentration in stratified river plumes using Thematic Mapper data. *International Journal of Remote Sensing*, 18(12), 2699–2705.

UNEP Assessment Report, Part I: The South Asian Haze: Air Pollution, Ozone and Aerosols, [Online] available: <http://www.rrcap.unep.org/issues/air/impactstudy/Part%20I.pdf>.

Ung, A., Weber, C., Perron, G., Hirsch, J., Kleinpeter, J., Wald, L. and Ranchin, T., 2001a. Air Pollution Mapping Over A City – Virtual Stations And Morphological Indicators. Proceedings of 10th International Symposium “Transport and Air Pollution” September 17 - 19, 2001 – Boulder, Colorado USA. [Online] available: http://www.cenerg.cma.fr/Public/themes_de_recherche/teledetection/title_tele_air/title_tele_air_pub/air_pollution_mappin4043.

Ung, A., Wald, L., Ranchin, T., Weber, C., Hirsch, J., Perron, G. and Kleinpeter, J., 2001b. , Satellite data for Air Pollution Mapping Over A City- Virtual Stations, Proceeding of the 21th EARSeL Symposium, Observing Our Environment From Space: New Solutions For A New Millenium, Paris, France, 14 – 16 May 2001, Gerard Begni Editor, A., A., Balkema, Lisse, Abingdon, Exton (PA), Tokyo, pp. 147 – 151, [Online] available: http://www.cenerg.cma.fr/Public/themes_de_recherche/teledetection/title_tele_air/title_tele_air_pub/atellite_data_for_t.

Vermote, E., Tanre, D., Deuze, J. L., Herman, M. and Morcrette, J. J., (1997) Second Simulation of the satellite signal in the solar spectrum (6S), [Online] available: http://www.geog.tamu.edu/klein/geog661/handouts/6s/6smanv2.0_P1.pdf

Weber, C., Hirsch, J., Perron, G., Kleinpeter, J., Ranchin, T., Ung, A. and Wald, L. 2001. Urban Morphology, Remote Sensing and Pollutants Distribution: An Application To The City of Strasbourg, France. International Union of Air Pollution Prevention and Environmental Protection Associations (IUAPPA) Symposium and Korean Society for Atmospheric Environment (KOSAE) Symposium, 12th World Clean Air & Environment Congress, Greening the New Millennium, 26 – 31 August 2001, Seoul, Korea. [Online] available: http://www.cenerg.cma.fr/Public/themes_de_recherche/teledetection/title_tele_air/title_tele_air_pub/paper_urban_morpho.